NACA RM A51D18

NACA

RESEARCH MEMORANDUM

EFFECTS OF DOUBLE-SLOTTED FLAPS AND LEADING-EDGE MODIFICATIONS ON THE LOW-SPEED CHARACTERISTICS OF A LARGE-SCALE 45° SWEPT-BACK WING WITH AND WITHOUT CAMBER AND TWIST

By Harry A. James and Joseph K. Dew

Ames Aeronautical Laboratory
Moffett Field, Calif.

NATIONAL ADVISORY COMMITTEE
FOR AERONAUTICS

WASHINGTON
July 23, 1951

NATIONAL ADVISORY COMMITTEE FOR AERONAUTICS

RESEARCH MEMORANDUM

EFFECTS OF DOUBLE-SLOTTED FLAPS AND LEADING-EDGE MODIFICATIONS ON THE LOW-SPEED CHARACTERISTICS OF A LARGE-SCALE 45° SWEPT-BACK WING WITH AND WITHOUT CAMBER AND TWIST

By Harry A. James and Joseph K. Dew

SUMMARY

An investigation has been conducted on two large-scale, semispan, wing-fuselage models with the 0.25-chord line swept back 45° to determine and compare the effects of partial-span, double-slotted flaps on the characteristics of a 45° swept-back wing with and without camber and twist. An investigation was also conducted to determine the effects of various full-span, leading-edge modifications on the characteristics of the models with and without double-slotted flaps.

The results show that partial-span, double-slotted flaps improved the high-lift and moment characteristics on both wing models. The improvements in maximum lift coefficient were from 0.9 to 1.2 for the wing with no camber and twist, and from 1.1 to 1.4 for the wing with camber and twist; corresponding increases in the lift coefficient at which large variations in force and moment characteristics took place were also realized. The increases, at zero angle of attack, in lift coefficient due to the double-slotted flaps were 0.62 for the wing with no camber and no twist, and 0.47 for the wing with camber and twist.

The results show that of the two wing models the one with camber and twist attained higher lift coefficients before the rate of drag rise increased abruptly, indicating that section stall was delayed to higher lift coefficients. The increase in this lift coefficient amounted to about 0.44 when the flaps were retracted and about 0.28 when the flaps were extended.

The best leading-edge modification on the wing without camber and twist increased the lift coefficient at which there was an abrupt increase in rate of drag rise with lift coefficient by about 0.23 for

the wing with flaps extended or retracted. For the cambered, twisted wing with flaps retracted there was practically no change. However, on this wing with flaps extended an increase of about 0.11 was realized.

The theory of NACA TN 2278, 1951, was satisfactory for predicting the lift increment, at 0° angle of attack, due to the double-slotted flaps. The wing lift coefficient at which large variations in the force and moment characteristics occurred corresponded approximately with the calculated onset of section stall.

INTRODUCTION

The application of camber and twist to a swept wing was first of interest as a means of improving high-speed performance. It became evident, however, that the use of camber and twist to distribute the wing load more uniformly at high speeds (low lift) would also improve the low-speed (high-lift) characteristics. Accordingly, an investigation at low speed was undertaken on a large-scale 45° swept-back wing of aspect ratio 6, taper ratio of 0.5, and cambered and twisted for a design lift coefficient of 0.4. The lift, drag, and pitching-moment characteristics of this wing and one of similar plan form but without camber and twist were reported in references 1 and 2. Since flaps are commonly employed to increase the lift at low speeds, an investigation of the effectiveness of flaps on the two wings was undertaken and is reported herein.

The particular choice of flap type and area distribution used in this investigation resulted from the following reasoning. While the camber and twist chosen on the basis of high-speed requirements gave some improvements in the high-lift characteristics, it was anticipated that at low speed more improvement could be realized from further increases in camber and twist. Additional camber, to increase further the section maximum lift of the thin sections, and increased twist, to counteract the induced effects of sweep, together would enable all sections of the wing to reach high lifts and more sections of the wing to reach their maximum lifts simultaneously. Such further increases in camber and twist at low speeds would be acceptable, of course, only if they could be eliminated at high speeds.

Trailing-edge flaps present a means of effectively varying camber and twist in flight. By use of the theory of reference 3, it is possible to design a flap installation which provides a specified span loading distribution, which might otherwise be obtained by wing camber and twist. Analysis based on references 3 and 4 shows that a rough approximation of such a flap installation can be realized with a flap of partial span, provided that the lift increment due to the flaps and the maximum lift

of the flapped section are both sufficiently great. Computed span loadings show that, with this sort of compromise, the two-dimensional maximum lift of sections just outboard of the flaps would have to be exceeded if significant gains in lift were to be realized. The analysis of reference 4 indicates that such a circumstance did exist for the flapped wing considered in that reference. For the wing plan form under study, double-slotted flaps extending from 0.2 semispan (wing-fuselage juncture) to 0.6 semispan were therefore chosen in order to obtain high flap-lift increments, high maximum section lifts, and an optimum utilization of available section maximum lift. The flap sections were chosen on the basis of data given in reference 5.

In addition to the tests described above, studies were also made of several leading-edge modifications which, based on the results of reference 2, were believed to offer the possibility of further improvements in the high-lift characteristics of the uncambered, untwisted wing. These included various changes in leading-edge radius and camber designed to delay or eliminate separation of air flow from the wing leading edge. The effect of increased leading-edge radius and camber was also investigated in the case of the cambered, twisted wing although the analysis of reference 2 indicated little or no gain would be expected.

NOTATION

The data are presented in the form of standard NACA coefficients which are applicable to a full-span configuration. Moments are referred to the quarter point of the mean aerodynamic chord[1] (fig. 1) and all coefficients are based on the dimensions[2] of the untwisted wing.

C_L lift coefficient $\left(\frac{L}{qS}\right)$

$C_{L_{sep}}$ lift coefficient at which rate of drag rise with lift suddenly increases

ΔC_{L_f} increment of lift coefficient due to flap deflection

---

[1]The mean aerodynamic chord is located in the wing reference plane defined by the quarter-chord line of the wing panel and the root chord line at the axis of symmetry.

[2]The projected area of the twisted wing at 0° angle of attack of the wing-root section was approximately 0.5 percent less than the area of the untwisted wing.

C_D drag coefficient $\left(\frac{D}{qS}\right)$

C_m pitching-moment coefficient $\left(\frac{M}{qS\bar{c}}\right)$

c_l section lift coefficient

c_{l_i} section ideal lift coefficient

$c_{l_{max}}$ maximum section lift coefficient

D drag on semispan wing, pounds

L lift on semispan wing, pounds

M pitching moment of semispan wing, foot-pounds

S area of semispan wing, square feet

b span of complete wing, feet

$\bar{c}$ mean aerodynamic chord $\left(\frac{\int_0^{b/2} c'^2 dy}{\int_0^{b/2} c' \, dy}\right)$, feet

c local chord measured perpendicular to the quarter-chord line

c' local chord measured parallel to plane of symmetry, feet

q dynamic pressure, pounds per square foot

y spanwise coordinate normal to plane of symmetry, feet

α angle of attack of wing root chord, degrees

ϵ angle of twist with respect to root chord (positive for washin), degrees

η fraction of semispan $\left(\frac{y}{b/2}\right)$

MODEL AND APPARATUS

The principal dimensions of the two semispan, wing–fuselage models used in this investigation are shown in figure 1. The wind-tunnel floor served as a reflection plane, and the models were supported on a turntable, independent of the tunnel-floor structure, in such a manner that only the aerodynamic forces and moments on the wing fuselage were measured on the wind-tunnel six-component balance system. There was a 1/4-inch gap between the fuselage and the tunnel floor. A view of the semispan test installation is shown in figure 2.

Except for differences of camber and twist, the two wings were similar in that they had 45° of sweepback of the quarter-chord line, an aspect ratio of 6, and a taper ratio of 0.5. The plain wing had an NACA 64A010 section normal to the quarter-chord line and had no twist and no camber. The cambered, twisted wing had an NACA 64A810, a=0.8 (modified) section normal to the quarter-chord line and was twisted over the span to give 10° washout (streamwise) at the tip as shown in figure 1. Coordinates of the airfoil sections, derived from reference 6, are presented in table I. The wing tips were formed by half-bodies having a local diameter equal to the corresponding thickness of the tip section. Further details of the design of the wings can be found in reference 1.

The fuselage shape was defined by a half-body of revolution with a fineness ratio of 4.9; details of the fuselage thickness distribution are presented in figure 1. The chord line of each wing at the plane of symmetry had zero incidence with respect to the fuselage center line.

The double-slotted flaps (hereinafter referred to simply as flaps) used in this investigation extended from 0.20 semispan to 0.60 semispan at which points the flaps were terminated along lines normal to the 75-percent-chord line. The main and foreflaps were 0.25 chord and 0.075 chord, respectively, measured normal to the quarter-chord line. The flap coordinates, chosen on the basis of results given in reference 5, are given in tables II and III. Detailed views of the flaps are shown in figure 3. The deflection angles for the main flap and the foreflap measured in a plane normal to the wing quarter-chord line were 55° and 30°, respectively.

The various modified airfoil sections are denoted 1, 2, 3, and 4 and are illustrated in figure 3. The coordinates of these sections are given in table I. Of note is the fact that the leading-edge radius of airfoil section 1 (0.011 chord) is equal to that of a 10-percent-thick NACA four-digit series airfoil. Each of the leading-edge modifications extended over the exposed span of the wing.

TESTS AND CORRECTIONS

Force tests of the two semispan models with the various high-lift devices were made through an angle-of-attack range from -8° through the angle of the maximum lift coefficient. The tests were all made at a Reynolds number of 8 million (based on a wing mean aerodynamic chord of 6.21 ft) which corresponds to a dynamic pressure of about 55 pounds per square foot and a Mach number of 0.2.

The following jet-boundary corrections, derived from reference 7 for a semispan unswept-wing installation without flaps, were added to the angle-of-attack and drag-coefficient data:

$$\Delta\alpha = 0.26\ C_L$$

$$\Delta C_D = 0.0045\ C_L^2$$

No corrections were made for the effect of the tunnel-floor boundary-layer air on the characteristics of the models or for the leakage through the clearance gap between the fuselage and the tunnel floor. Measurements of the total thickness of the boundary layer on the tunnel floor (at the model location) and on top of the fuselage (near the leading-edge of the wing) revealed the thicknesses to be of the order of 14 inches and 1 inch, respectively, for the test conditions of this investigation.

RESULTS AND DISCUSSION

The lift, drag, and pitching-moment characteristics of the two semispan wing-fuselage models are presented in figures 4, 5, and 6. The configurations consist of the models with and without flaps in combination with various leading-edge modifications. Figures 7 and 8 contain the lift-drag-ratio variations and the drag characteristics; the latter are presented in a manner to show the relative gliding and sinking speeds of the various configurations at sea level, based on a wing loading of 50 pounds per square foot.

It should be noted that the data in figure 4 for the wings without flaps are from reference 1. These data were obtained from tests made prior to the trailing-edge modification to accommodate the flaps. They are considered to be more representative of the clean configurations since the profile of the wing with flaps retracted deviated somewhat from the original profile.

Lift and Pitching-Moment Characteristics

Effects of the flaps on the characteristics of the plain wing.- In figure 4, it may be seen that the effects of the flaps on the lift characteristics of the plain wing at 0° angle of attack were to increase the lift coefficient from 0 to 0.62 and to reduce the lift-curve slope from 0.059 to 0.056. The lift-curve slope for the wing with flaps extended was essentially linear up to a lift coefficient of about 1.00 at which point the slope began to decrease, marking the beginning of important changes in the pitching-moment and drag characteristics (to be discussed later in this report). The slope continued to decrease as the lift increased, resulting in a rounded lift-curve peak as the maximum lift coefficient of 1.20 was reached. This value represents a gain in maximum lift coefficient of about 0.30 due to the flaps.

The effects of the flaps on the pitching-moment characteristics of the plain wing were to cause (1) a pitching-moment-coefficient increment of -0.13 to -0.14 throughout the lift-coefficient range where the pitching-moment coefficient varied linearly with lift coefficient, (2) a $0.01\bar{c}$ rearward shift of the aerodynamic center, and (3) an extension of the linear portion of the pitching-moment curve from a lift coefficient of 0.65 to 1.00. At higher lift coefficients, extreme instability occurred.

Effects of the flaps on the characteristics of the cambered, twisted wing.- In figure 4 it can be seen that the effects of the flaps on the lift characteristics of the cambered, twisted wing at 0° angle of attack were to increase the lift coefficient from 0.02 to 0.49 and to reduce the lift-curve slope from 0.060 to 0.055. The lift curve for this wing was essentially linear over the entire lift range.[3] The maximum lift coefficient of this wing with flaps was about 1.39. This value represents a gain in maximum lift coefficient of about 0.30 due to the flaps.

The flap lift increment (0.47) at 0° angle of attack was 0.15 less than for the plain wing even though the section profiles of the wings differed only by the shape of their mean camber lines. Visual tuft studies indicated rougher air flow over the flaps on the cambered, twisted wing than on the plain wing, which could be indicative of unsteady flow and separation resulting from excessive flap deflection or nonoptimum slot design. The 55° deflection used for these tests was

[3]Deviation is confined to a normally unimportant low-lift range for a flapped wing (below a C_L of 0.25), in which the longitudinal characteristics of the cambered, twisted wing exhibited changes suggestive of lower-surface flow separation as explained in reference 2.

based on the best deflection and slot design for a section cambered for an ideal lift coefficient of 0.2 (reference 5) and therefore may not have been optimum for this highly cambered section. The shape of the after portion of the NACA 64A810 section resembles the symmetrical section with the main flap deflected 10°, and thus, with the addition of a flap deflected 55°, the effective flap deflection may have been about 65°.

The effects of the flaps on the pitching-moment characteristics of the cambered, twisted wing were to cause (1) a pitching-moment coefficient change of about −0.08 at the wing design lift coefficient of 0.40, (2) a $0.01\bar{c}$ forward shift of the aerodynamic center, and (3) an extension of the near linear portion of the pitching-moment curve from a lift coefficient of 0.80 to 1.30. Above a lift coefficient of 1.00, a gradual forward shift of the aerodynamic center occurred similar to the aerodynamic-center shift on the unflapped wing above a lift coefficient of 0.80. This shift was explained in reference 2 as being due to a progressive increase in trailing-edge separation on the outboard section of the wing. At the maximum lift coefficient severe instability occurred.

Effects of leading-edge modifications.- Since a leading-edge type of flow separation was found to be the factor fixing the value of the lift coefficient at which marked changes occurred in the characteristics for the plain wing (reference 2), the leading-edge radius of the wing was increased from 0.007 chord to 0.011 chord (airfoil section 1) and to 0.015 chord (airfoil section 2). The increased leading-edge radii were so placed that the arcs were tangent to the upper-surface contour and that a curve tangent to the leading-edge arc could be faired smoothly into the lower-surface contour of the NACA 64A010 section, thus introducing a small amount of camber near the leading edge of the section. (See fig. 3.) Airfoil section 1 had a theoretical c_{l_i} of approximately 0.1. Airfoil section 2 had a theoretical c_{l_i} of approximately 0.3. An additional modification was made (airfoil section 3) whereby the 0.015-chord radius was placed in a manner which resulted in an increase in the forward camber and gave a theoretical c_{l_i} of 0.6.

In figure 5 are shown the effects of the leading-edge modifications on the aerodynamic characteristics of the plain wing. It may be noted that the data in figure 5(a) for the wing with unmodified leading edge and with flaps retracted differs slightly from the data for the plain wing with no trailing-edge flaps which is presented in figure 4. It is presumed that this difference is attributable to a small change in the section contour which occurred as a result of the flap installation. Since this discrepancy in airfoil contour was common to the various configurations with leading-edge modifications, it is believed that the incremental results were not affected by it.

Figures 5(a) and 5(b) show the effects of the modifications on the plain wing with and without flaps. In the low-to-moderate lift range, the only noteworthy effect was a slight positive increment in pitching-moment coefficient which may have been due to a change in the spanwise load since it is in the opposite direction to what would be expected from two-dimensional considerations. The effects of the modifications were of a more significant magnitude in the upper lift range. Each of the modifications increased the near-linear portion of the pitching-moment curve to a higher lift coefficient. With the flaps retracted, the increments in lift coefficient were 0.10, 0.10, and 0.17 for the airfoil sections 1, 2, and 3, respectively. With flaps extended, the respective increments were 0.16, 0.21, and 0.34. Increases in $C_{L_{max}}$ were also obtained by use of airfoil sections 1, 2, and 3, respectively; they were 0.03, 0.04, and 0.12 when the flaps were retracted, and 0.05, 0.06, and 0.16 when the flaps were extended.

The 0.015-chord-radius leading-edge modification was tested on the cambered, twisted wing (airfoil section 4) to determine if any improvement in the flow over the leading edge of the highly cambered section could be achieved by such an enlargement of the leading-edge radius and increase in leading-edge camber. The results for this wing with flaps retracted are shown in figure 6(a). In the low-lift range, the pitching-moment curve has been noticeably straightened out. This may be due to alleviation of lower-surface separation over the leading-edge portion of the wing, known to exist on this wing (reference 2). As would be expected on the basis of the results of reference 2, wherein it was indicated that for this wing no serious leading-edge flow-separation problem existed at moderate to high lift coefficients, the effects of the enlarged leading-edge radius on the wing with flaps retracted were negligible. For the wing with flaps, however, the value of $C_{L_{max}}$ was increased by about 0.10 with a corresponding extension of the near-linear portion of the pitching-moment curve to a higher lift coefficient (fig. 6(b)).

Drag Characteristics

The basic drag data of both models with and without flaps and with the various leading-edge modifications are presented in figures 4, 5, and 6, and together with the lift-drag ratio (L/D) as a function of lift coefficient in figures 7 and 8.

Drag and lift-drag ratio.- The drag characteristics of both wings in the clean configuration (from reference 1) are included in figure 7(a) for the purpose of evaluating the effect of the flaps. At a lift coefficient of 0.40 the incremental drag coefficients due to flaps were

0.050 and 0.065 for the plain wing and the cambered, twisted wing, respectively. The greater incremental drag measured on the cambered, twisted wing is believed to be related to unsteady flow and separation resulting from the nonoptimum flap setting as pointed out earlier. Both models with flaps have essentially constant lift–drag ratios between a lift coefficient of 0.80 and the lift coefficient at which the rate of drag rise with lift suddenly increases. The greater rate of increase is believed to be indicative of the beginning of stall on the wing. For convenience, the lift coefficient at which it occurs will be referred to hereinafter as $C_{L_{sep}}$. A maximum lift–drag ratio of 8.0 was obtained at a lift coefficient of 1.20 for the cambered, twisted wing with flaps extended, as compared to a maximum lift–drag ratio of 8.4 at a lift coefficient of 1.05 for the plain wing with flaps extended. It is interesting to note that at this value of lift coefficient (1.05) the cambered, twisted wing in the clean condition had a higher value of lift–drag ratio than the plain wing with flaps extended.

In general, the leading–edge modifications (figs. 5 and 6) produced negligible effects on the drag characteristics at low and moderate lift coefficients. However, in the high lift range, the point of sudden increase in the rate of drag rise with lift coefficient was shifted to higher values of lift coefficient. These higher values of $C_{L_{sep}}$ correspond to the highest values of lift coefficient attained before the beginning of sharp reductions in lift–drag ratio.

In figure 8, the drag characteristics and lift–drag ratio of the modified plain wing (airfoil section 3) are compared to the characteristics of the modified cambered, twisted wing (airfoil section 4). The best modification on the plain wing resulted in higher values of L/D for lift coefficients below $C_{L_{sep}}$ as compared to those of the modified cambered, twisted wing; however, the cambered, twisted wing with the flaps either retracted or extended attained a higher value of $C_{L_{sep}}$ than did the corresponding plain wing configurations.

Power–off glide.– The drag polars in figures 7 and 8 have a superimposed grid of power–off glide and sinking speeds computed for sea–level conditions and a wing loading of 50 pounds per square foot. For convenience of comparison between the configurations tested, the following table summarizes the relative glide and sinking speeds corresponding to the values of $C_{L_{sep}}$:

Configuration	Fig. no.	$C_{L_{sep}}$	Sinking speed (ft/sec)	Gliding speed (mph)
Plain wing	7(a)	0.65	16	173
Cambered, twisted wing	7(a)	1.09	18	135
Plain wing, flaps extended	7(a)	1.08	22	134
Cambered, twisted wing, flaps extended	7(a)	1.36	21	119
Plain wing, airfoil section 2	7(b)	.84	17	152
Cambered, twisted wing, airfoil section 4	7(b)	1.09	18	133
Plain wing, airfoil section 2, flaps extended	7(b)	1.21	21	128
Cambered, twisted wing, airfoil section 4, flaps extended	7(b)	1.47	21	116
Plain wing, airfoil section 3	8	.88	17	149
Plain wing, airfoil section 3, flaps extended	8	1.31	21	122

Comparison of Theory With Experiment for Both Models

The theoretical values of the lift increment at 0° angle of attack due to the flaps and the theoretical values of the lift coefficient at which initial section stall would occur have been compared to the corresponding experimental values. In the computation of the lift increments due to the flaps, no attempt was made to account for the effect of the fuselage on the variation of wing load. Accordingly, the theoretical computations for the subject tests were based on the actual span of the flaps. The predicted lift increment due to the flaps given by the method of reference 3 was 0.57 for each wing as compared to 0.62 and 0.47 measured for the plain wing and the cambered, twisted wing, respectively.

The method of reference 4 has been applied to ascertain theoretically, for the subject wings, the wing lift coefficient at which the first section reached maximum lift and the spanwise point where this occurred. Maximum lift coefficients for the unflapped sections were obtained from reference 6 and reference 8; maximum lift coefficients for the flapped sections were estimated from the data given in

reference 5 for a section with a c_{l_i} of 0.2. These estimates may be somewhat in error, particularly for the NACA 64A810 section, because of the differences in design lift coefficients. Figures 9(a) and 9(b) illustrate the results of applying the method of reference 4. From these figures it would be predicted that initial section stall would appear at a C_L of 1.0 for the plain wing with flaps and at a C_L of 1.2 for the cambered, twisted wing with flaps; the experimental drag results indicated values of $C_{L_{sep}}$ of approximately 1.1 and 1.4, respectively. The position of initial section stall is indicated to be near the outboard end of the flaps for both wings. Outboard of the flaps, the proximity of the curve of computed section lift coefficient to the curve of theoretical maximum section lift coefficient indicates that stall would progress rapidly toward the tips. The variations in the drag and pitching-moment data along with visual tuft observations seem to confirm these deductions.

CONCLUSIONS

From the results of an investigation at low speed of the effectiveness of the partial-span, double-slotted flaps and of camber and twist on the force and moment characteristics of a large-scale wing swept back 45°, with and without the various leading-edge modifications, the following conclusions may be drawn:

1. Partial-span, double-slotted flaps were an effective means of obtaining improved high-lift characteristics on the swept wings with and without camber and twist.

2. The combinations of increased leading-edge radius and nose camber were effective in delaying the onset of leading-edge flow separation to higher wing-lift coefficients.

3. Theory was satisfactory for predictions of the lift increment at 0° angle of attack due to the double-slotted flaps.

4. Theoretical predictions of the lift coefficient at which large variations in force and moment characteristics could be expected were in approximate agreement with experimental results.

Ames Aeronautical Laboratory,
National Advisory Committee for Aeronautics,
Moffett Field, Calif.

REFERENCES

1. Hunton, Lynn W.: Effects of Twist and Camber on the Low-Speed Characteristics of a Large-Scale 45° Swept-Back Wing. NACA RM A50A10, 1950.

2. Hunton, Lynn W., and Dew, Joseph K.: The Effects of Camber and Twist on the Aerodynamic Loading and Stalling Characteristics of a Large-Scale 45° Swept-Back Wing. NACA RM A50J24, 1951.

3. DeYoung, John: Theoretical Symmetric Span Loading Due to Flap Deflection for Wings of Arbitrary Plan Form at Subsonic Speeds. NACA TN 2278, 1951.

4. Maki, Ralph L.: The Use of Two-Dimensional Section Data to Estimate the Low-Speed Wing Lift Coefficient at Which Section Stall First Appears on a Swept Wing. NACA RM A51E15, 1951.

5. Cahill, Jones F., and Racisz, Stanley F.: Wind-Tunnel Investigation of Seven Thin NACA Airfoil Sections to Determine Optimum Double-Slotted-Flap Configurations. NACA TN 1545, 1948.

6. Loftin, Laurence K., Jr.: Theoretical and Experimental Data for a Number of NACA 6A-Series Airfoil Sections. NACA Rep. 903, 1948. (Formerly NACA TN 1368, 1947)

7. Glauert, H.: The Elements of Aerofoil and Airscrew Theory. The MacMillan Company, N.Y., 1943.

8. McCullough, George B., and Haire, William M.: Low-Speed Characteristics of Four Cambered, 10-Percent-Thick NACA Airfoil Sections. NACA TN 2177, 1950.

TABLE I.- COORDINATES OF THE AIRFOIL SECTIONS

[Stations and ordinates given in percent of airfoil chord]

(a) NACA 64A010

Station	Ordinate
0	0
.5	.804
.75	.969
1.25	1.225
2.5	1.688
5	2.327
7.5	2.805
10	3.199
15	3.813
20	4.272
25	4.606
30	4.837
35	4.968
40	4.995
45	4.894
50	4.684
55	4.388
60	4.021
65	3.597
70	3.127
75	2.623
80	2.103
85	1.582
90	1.062
95	.541
100	.021
L.E. radius = 0.687 T.E. radius = 0.023	

TABLE I.- CONTINUED

[Stations and ordinates given in percent of airfoil chord]

(b) NACA 64A810 (a = 0.8 modified)

Upper surface		Lower surface	
Station	Ordinate	Station	Ordinate
0	0	0	0
.214	.976	.785	-.526
.428	1.231	1.072	-.597
.881	1.650	1.619	-.686
2.064	2.475	2.936	-.787
4.506	3.716	5.494	-.832
6.984	4.703	8.016	-.811
9.479	5.541	10.521	-.771
14.500	6.902	15.500	-.658
19.543	7.968	20.457	-.526
24.601	8.795	25.399	-.383
29.668	9.420	30.332	-.232
34.742	9.857	35.258	-.065
39.820	10.107	40.180	.123
44.900	10.150	45.100	.364
49.977	10.005	50.023	.637
55.049	9.693	54.951	.917
60.114	9.225	59.886	1.187
65.169	8.612	64.831	1.426
70.215	7.850	69.785	1.610
75.252	6.932	74.748	1.710
80.300	5.819	79.700	1.657
85.292	4.441	84.708	1.331
90.204	3.004	89.796	.920
95.104	1.512	94.896	.450
100.000	.021	100.000	-.021

L.E. radius = 0.687
T.E. radius = 0.023

TABLE I.- CONTINUED

[Stations and ordinates given in percent of airfoil chord]

(c) Airfoil Section No. 1

Station	Ordinate	
	Upper	Lower
0	- - -	- - -
.5	0.804	- - -
.75	.969	- - -
1.25	1.225	-1.430
2.5	1.688	-1.750
5	2.327	
7.5	2.805	
10	3.199	
15	3.813	
20	4.272	
25	4.606	
30	4.837	
35	4.968	
40	4.995	
45	4.894	
50	4.684	
55	4.388	
60	4.021	
65	3.597	
70	3.127	
75	2.623	
80	2.103	
85	1.582	
90	1.062	
95	.541	
100	.021	

L.E. radius = 1.100
T.E. radius = 0.023
L.E. radius center:
station = 1.1; ordinate = -0.2

Note: Ordinates from stations 5 to 100 are identical to the NACA 64A010 airfoil section.

TABLE I.- CONTINUED

[Stations and ordinates given in percent of airfoil chord]

(d) Airfoil Section No. 2

Station	Ordinate	
	Upper	Lower
0	- - -	- - -
.5	0.804	- - -
.75	.959	- - -
1.25	1.225	- - -
2.5	1.688	-2.070
5	2.327	-2.380
7.5	2.805	
10	3.199	
15	3.813	
20	4.272	
25	4.606	
30	4.837	
35	4.968	
40	4.995	
45	4.894	
50	4.684	
55	4.388	
60	4.021	
65	3.597	
70	3.127	
75	2.623	
80	2.103	
85	1.582	
90	1.062	
95	.541	
100	.021	

L.E. radius = 1.500
T.E. radius = 0.023
L.E. radius center:
station = 1.3; ordinate = 0.4

Note: Ordinates from stations 7.5 to 100 are identical to the NACA 64A010 airfoil section.

TABLE I.- CONTINUED

[Stations and ordinates given in percent of airfoil chord]

(e) Airfoil Section No. 3

Station	Ordinate	
	Upper	Lower
0	- - -	- - -
.5	0.804	- - -
.75	.969	- - -
1.25	1.225	- - -
2.5	1.688	-1.630
5	2.327	-1.525
7.5	2.805	
10	3.199	
15	3.813	
20	4.272	
25	4.606	
30	4.837	
35	4.968	
40	4.995	
45	4.894	
50	4.684	
55	4.388	
60	4.021	
65	3.597	
70	3.127	
75	2.623	
80	2.103	
85	1.582	
90	1.062	
95	.541	
100	.021	

L.E. radius = 1.500
T.E. radius = 0.023
L.E. radius center:
station = 0.8; ordinate = -1.7

Note: Ordinates from station 7.5 to 100 are identical to the NACA 64A010 airfoil section.

TABLE I.- CONCLUDED

[Stations and ordinates given in percent of airfoil chord]

(f) Airfoil Section No. 4

Upper		Lower	
Station	Ordinate	Station	Ordinate
0	- - -	0	- - -
.214	0.976	2.500	-1.400
.428	1.231	5.000	-1.015
.881	1.650	8.016	-.811
2.064	2.475	10.521	-.771
4.506	3.716	15.500	-.658
6.984	4.703	20.457	-.526
9.479	5.541	25.399	-.383
14.500	6.902	30.332	-.232
19.543	7.968	35.258	-.065
24.601	8.795	40.180	.123
29.668	9.420	45.100	.364
34.742	9.857	50.023	.637
39.820	10.107	54.951	.917
44.900	10.150	59.886	1.187
49.977	10.005	64.831	1.426
55.049	9.693	69.785	1.610
60.114	9.225	74.748	1.710
65.169	8.612	79.700	1.657
70.215	7.850	84.708	1.331
75.252	6.932	89.796	.920
80.300	5.819	94.896	.450
85.292	4.441	100.000	-.021
90.204	3.004		
95.104	1.512		
100.000	.021		

L.E. radius = 1.500
T.E. radius = 0.023
L.E. radius center:
station = 1.4; ordinate = 0

Note: Ordinates from station 8.016 to 100 are identical to the NACA 64A810 a = 0.8 (mod.)

TABLE II.- ORDINATES FOR 0.25-CHORD FLAP

[Stations and ordinates given from airfoil chord line in percent airfoil chord]

(a) Plain Wing Flap

Station	Upper Ordinate	Lower Ordinate
75.000	-1.000	-1.000
75.150	-.371	-1.557
75.295	-.076	-1.712
75.587	.268	-1.956
75.882	.535	-2.095
76.177	.751	-2.179
76.765	1.057	-2.289
77.352	1.272	-2.320
77.942	1.414	-2.304
78.530	1.496	-2.260
79.705	1.594	-2.136
80.882	1.637	-2.003
82.060	1.648	-1.880
83.235	1.630	-1.762
84.410	1.583	-1.641
85.000	1.550	-1.582
86.250	1.453	-1.453
90.000	1.062	-1.062
95.000	.541	-.541
100.000	.021	-.021
L.E. radius = 0.95 (center on flap chord line)		
T.E. radius = 0.023		

TABLE II.- CONCLUDED

[Stations and ordinates given from airfoil chord line in percent airfoil chord]

(b) Cambered, Twisted Wing Flap

Upper		Lower	
Station	Ordinate	Station	Ordinate
74.900	3.330	-.100	3.330
75.130	3.930	.010	2.770
75.290	4.168	.130	2.580
75.620	4.553	.430	2.350
75.940	4.806	.680	2.187
76.280	4.994	.980	2.052
76.880	5.232	1.540	1.900
77.530	5.383	2.060	1.814
78.140	5.452	2.660	1.744
78.740	5.460	3.240	1.706
79.930	5.372	4.410	1.668
81.140	5.223	5.560	1.620
82.340	5.040	6.740	1.539
83.530	4.820	7.930	1.480
84.700	4.569	9.120	1.394
85.290	4.433	9.708	1.351
86.000	4.250	14.796	.920
90.204	3.004	19.896	.450
95.104	1.512	25.000	-.021
100.000	.021		

L.E. radius = 0.95 (center on flap chord line)
T.E. radius = 0.023

TABLE III.- ORDINATES FOR 0.075-CHORD FOREFLAP

[Stations and ordinates given from foreflap chord line in percent airfoil chord]

Plain Wing or Cambered, Twisted Wing Foreflap		
Station	Upper ordinate	Lower ordinate
0	0	0
.42	.95	-.93
.83	1.31	-1.14
1.25	1.52	-1.20
1.67	1.67	-1.11
2.08	1.72	-.85
2.92	1.74	-.36
3.75	1.64	-.02
4.58	1.43	.18
5.42	1.13	.27
6.25	.75	.25
7.08	.28	.11
7.50	0	0
L.E. radius = 1.20 (center on flap chord line)		

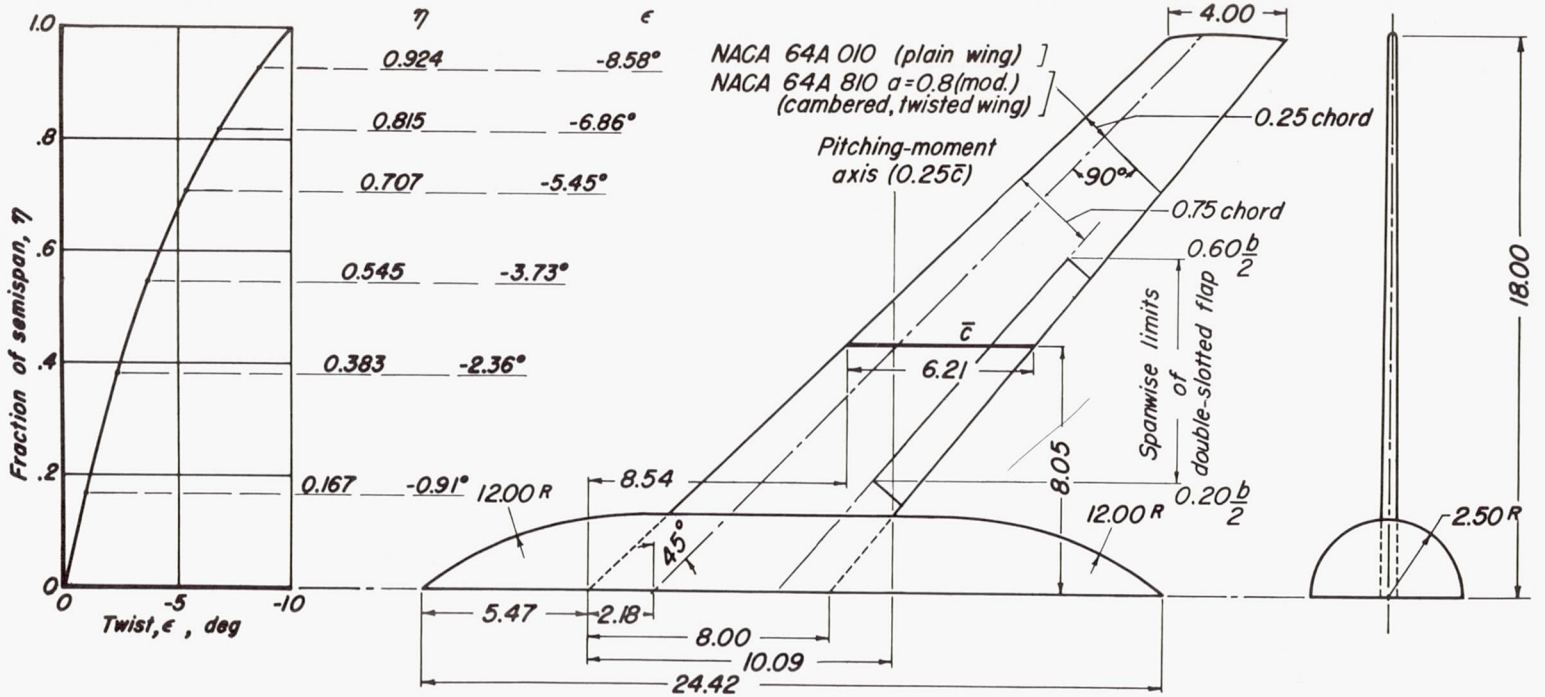

Note: All dimensions are in feet unless otherwise specified

Figure 1.- Dimensions of the semispan wing-fuselage models.

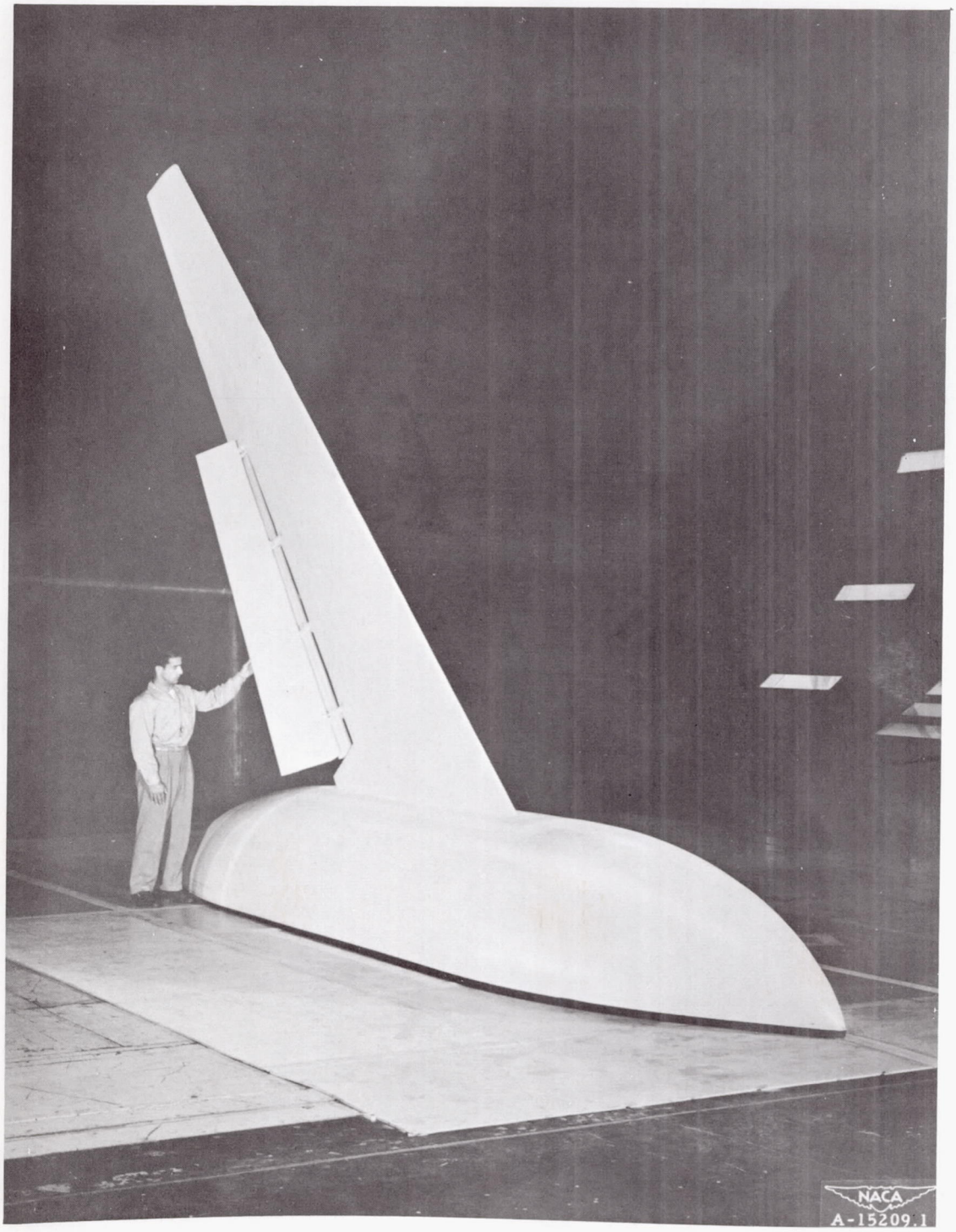

Figure 2.– Photograph of the semispan model installation in the Ames 40– by 80–foot wind tunnel.

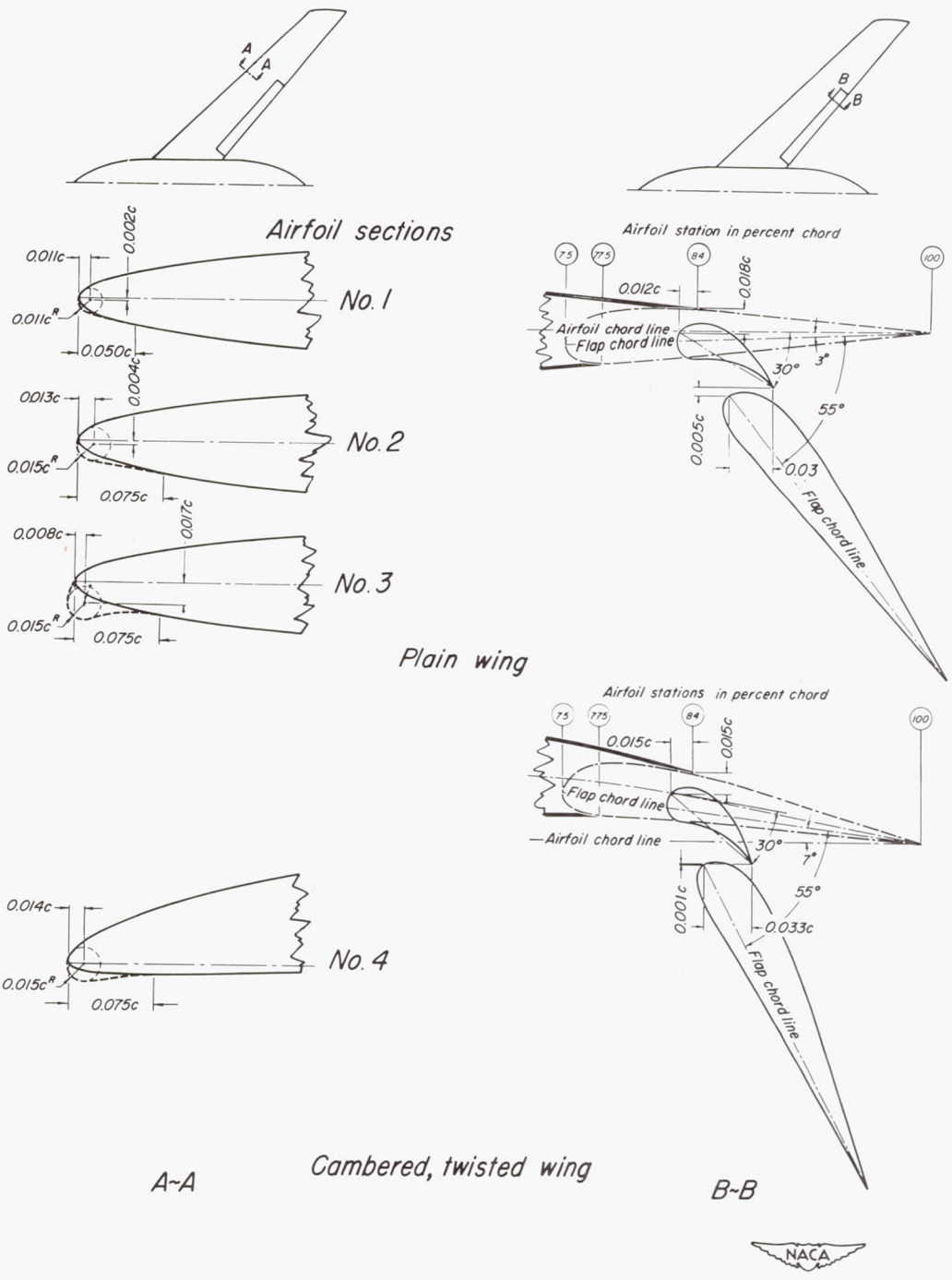

Figure 3.– Dimensions of the double–slotted flaps and the leading–edge modifications.

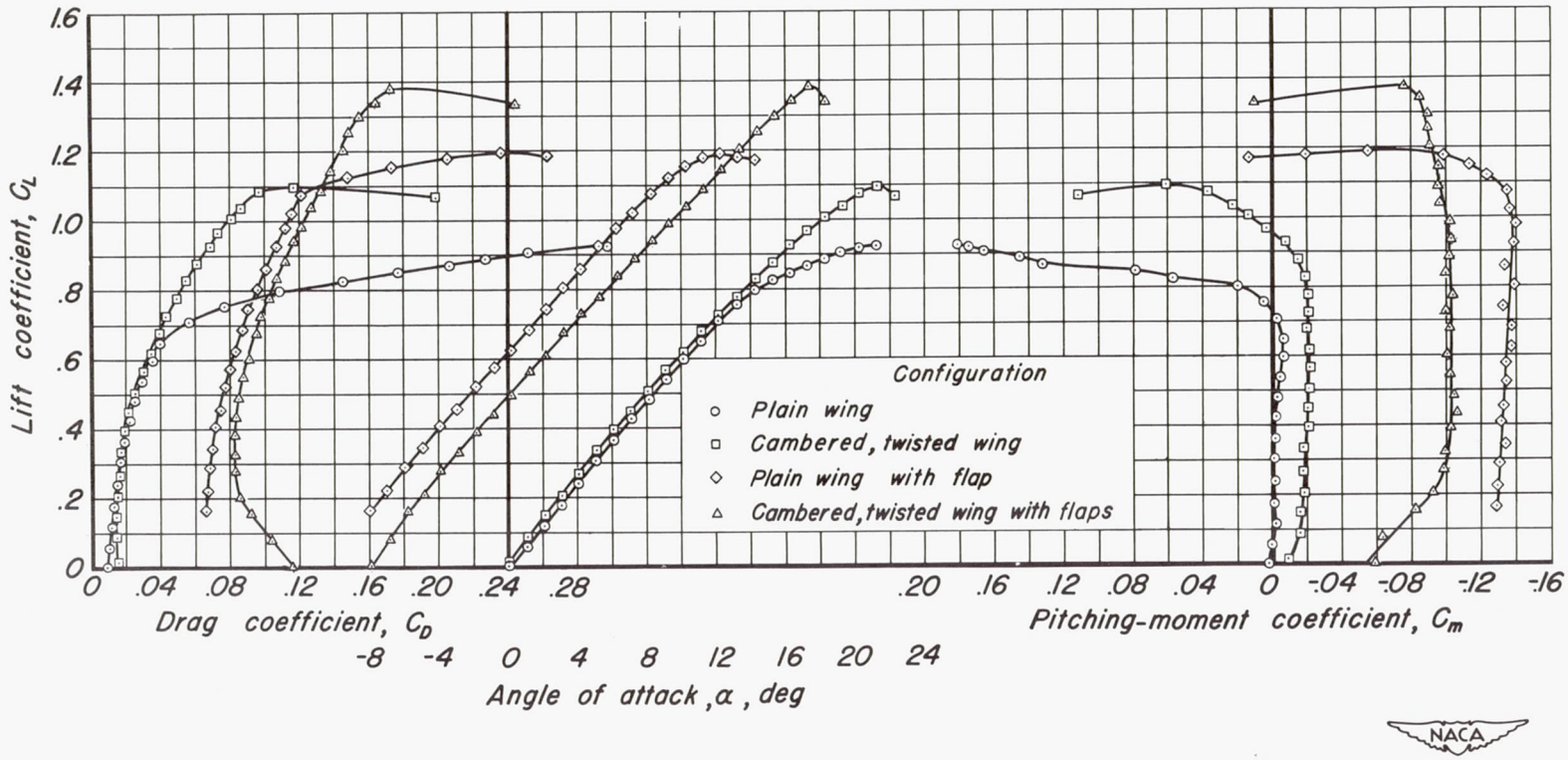

Figure 4.- The aerodynamic characteristics of the plain wing and the cambered, twisted wing models with and without double-slotted flaps.

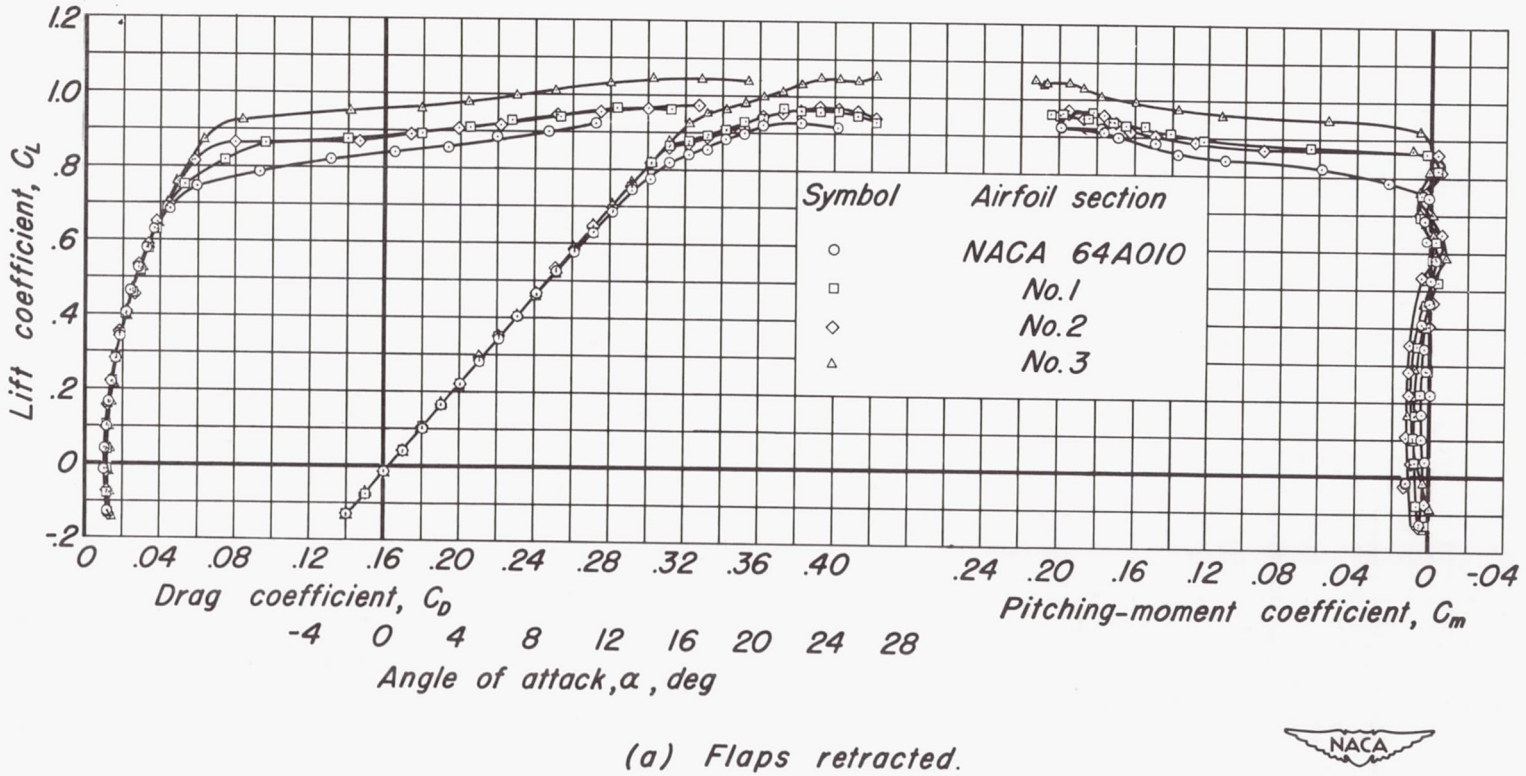

Figure 5.- Effects of the various leading-edge modifications on the aerodynamic characteristics of the plain wing model.

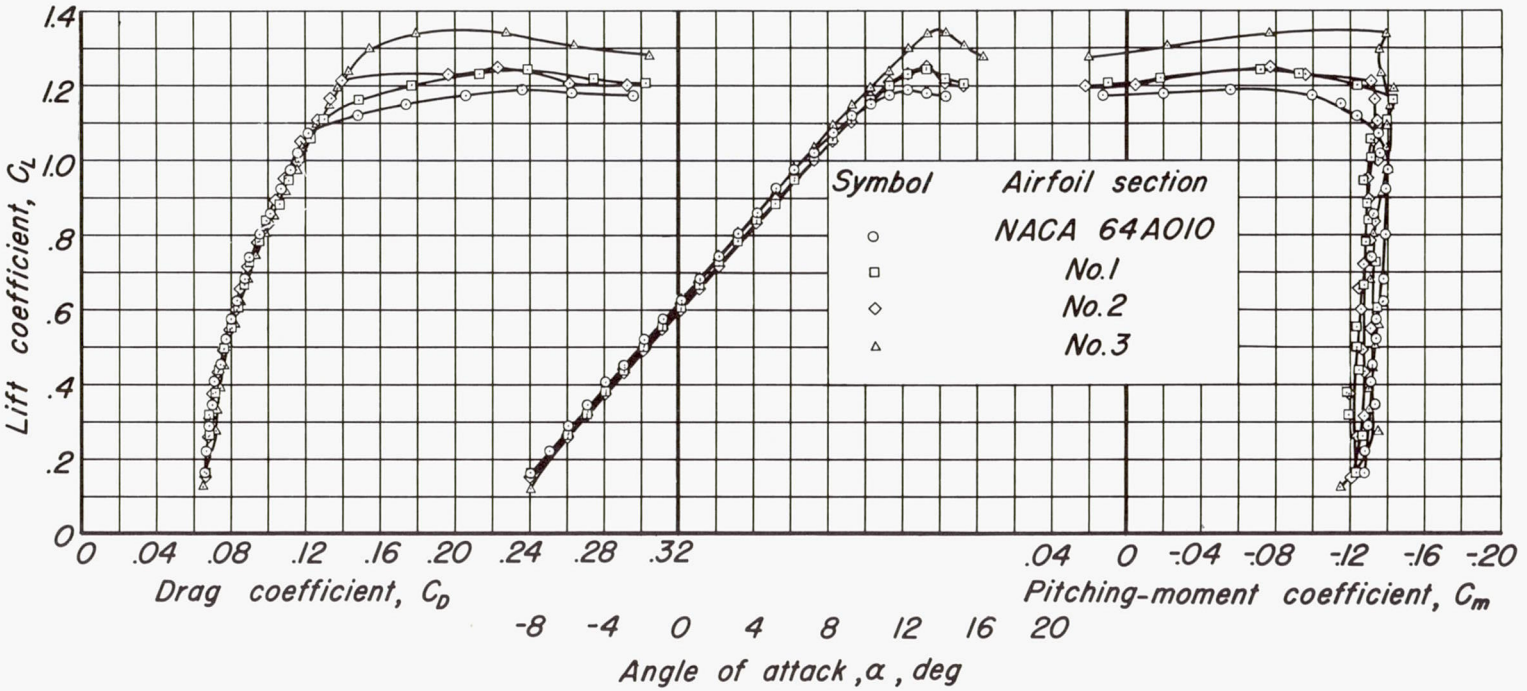

(b) Flaps extended.

Figure 5.- Concluded.

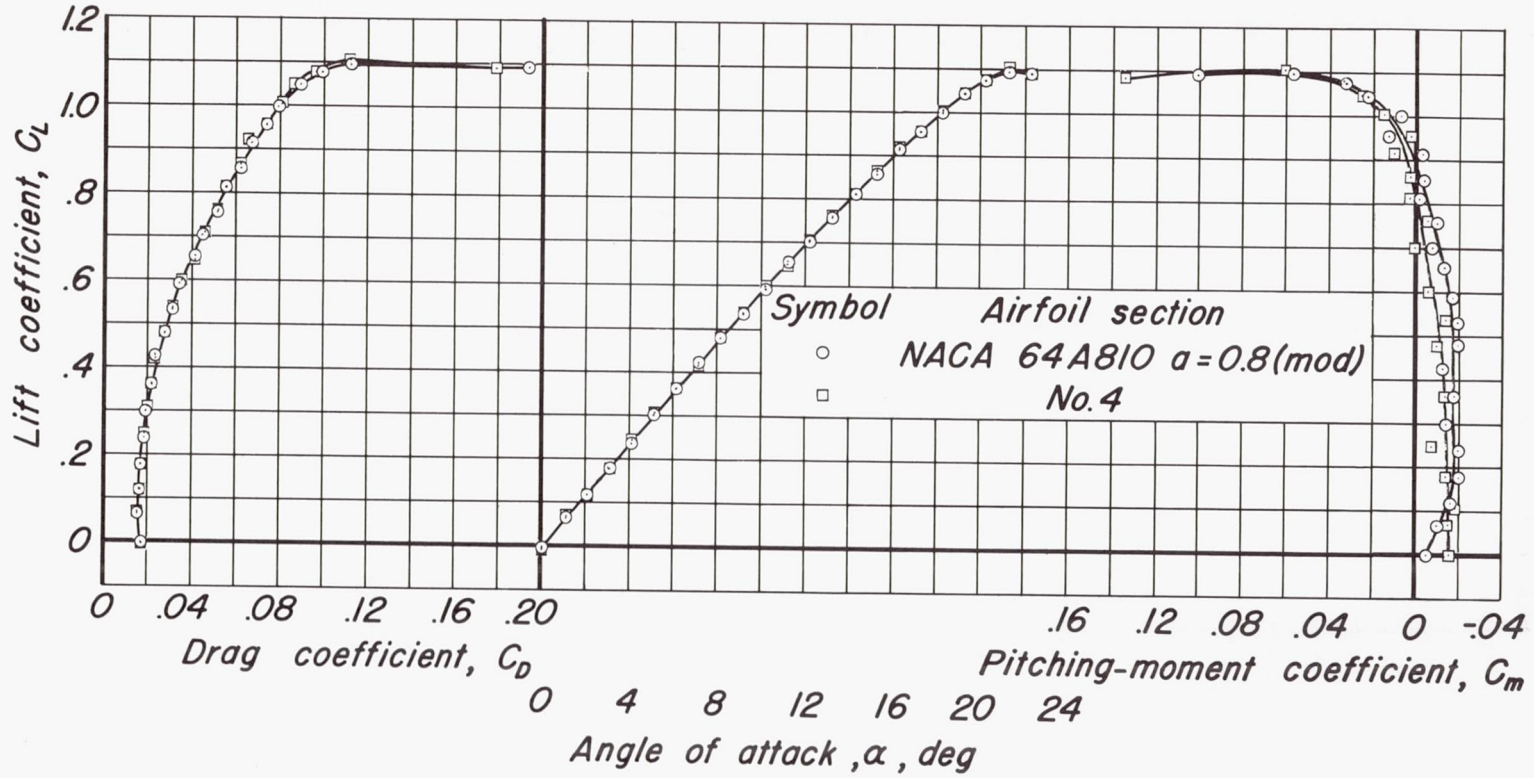

(a) Flaps retracted.

Figure 6.– Effects of the 0.015c leading-edge radius modification on the aerodynamic characteristics of the cambered, twisted wing model.

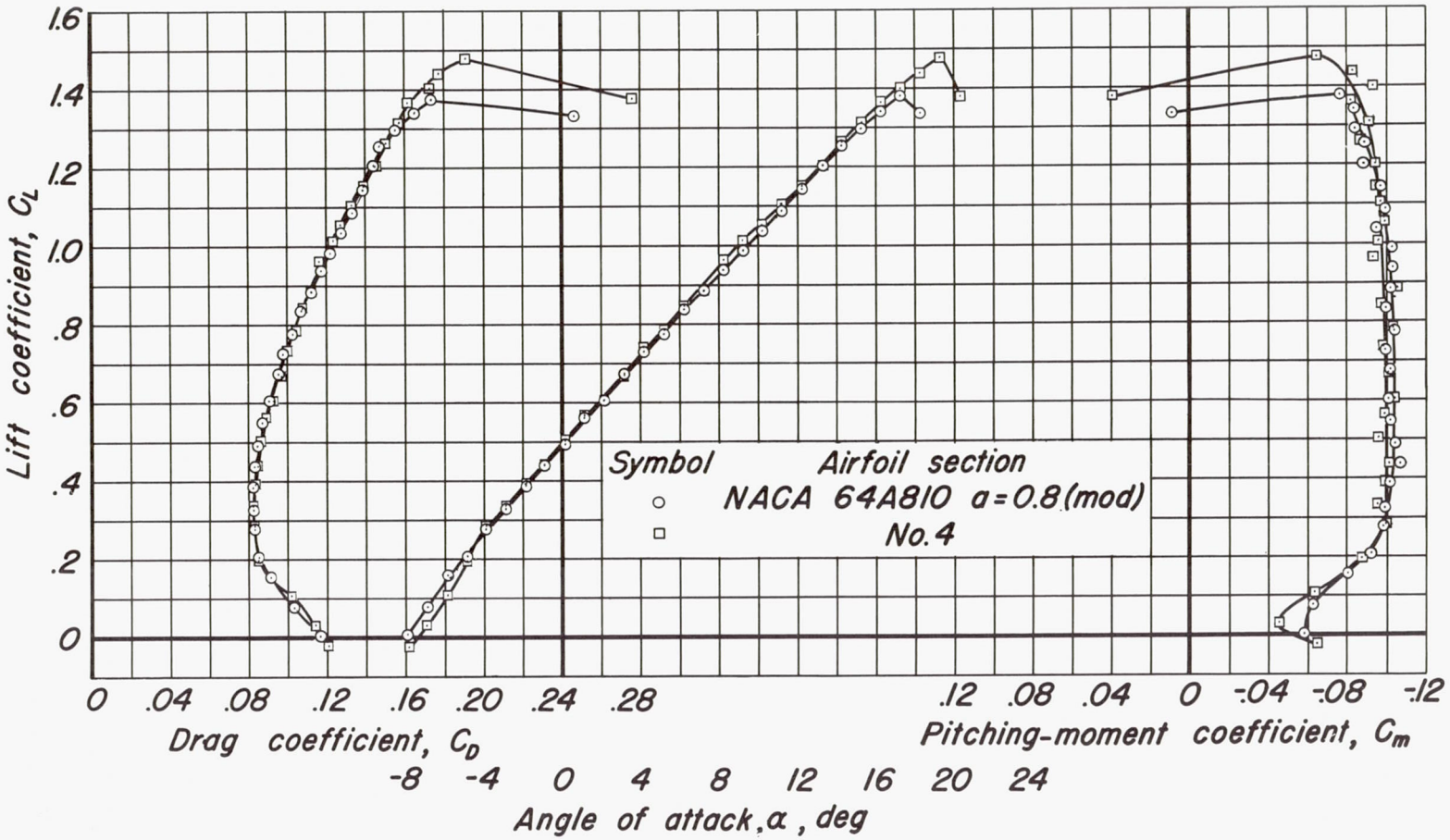

(b) Flaps extended.

Figure 6.- Concluded.

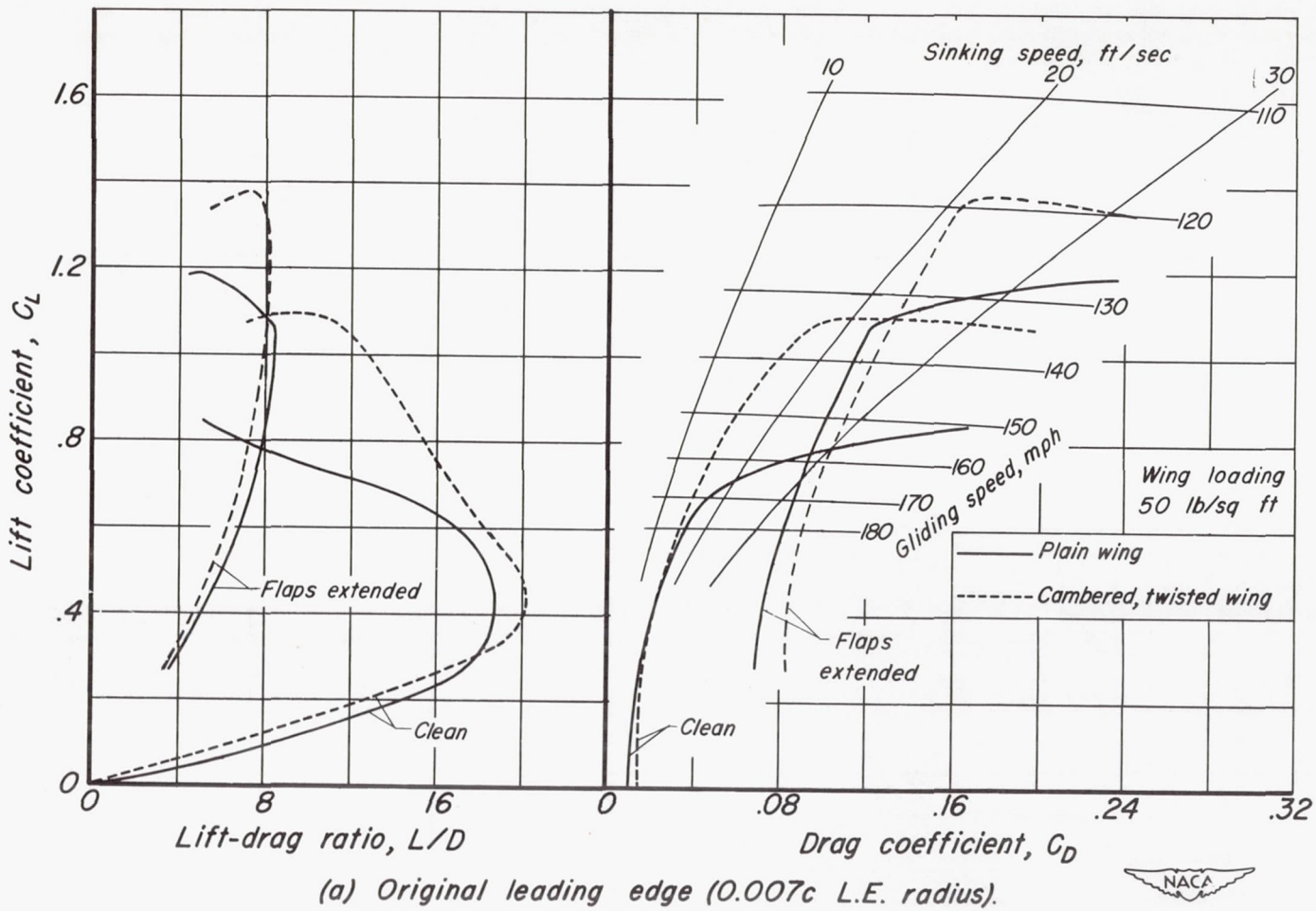

(a) Original leading edge (0.007c L.E. radius).

Figure 7.- The lift-drag ratio and power-off glide characteristics of the plain and cambered, twisted wing models with and without double-slotted flaps.

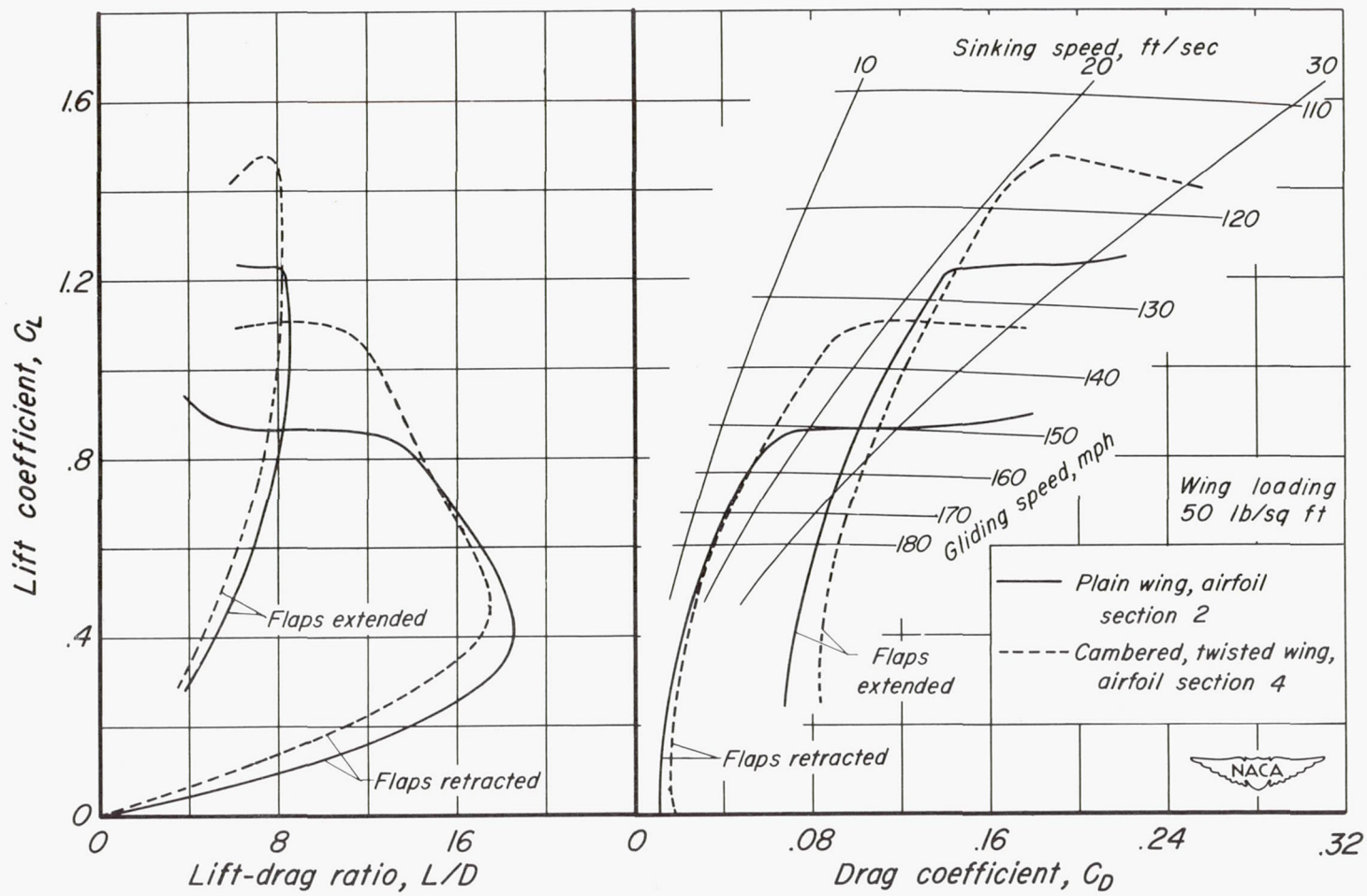

(b) Modified leading edge (0.015c L.E. radius).

Figure 7.– Concluded.

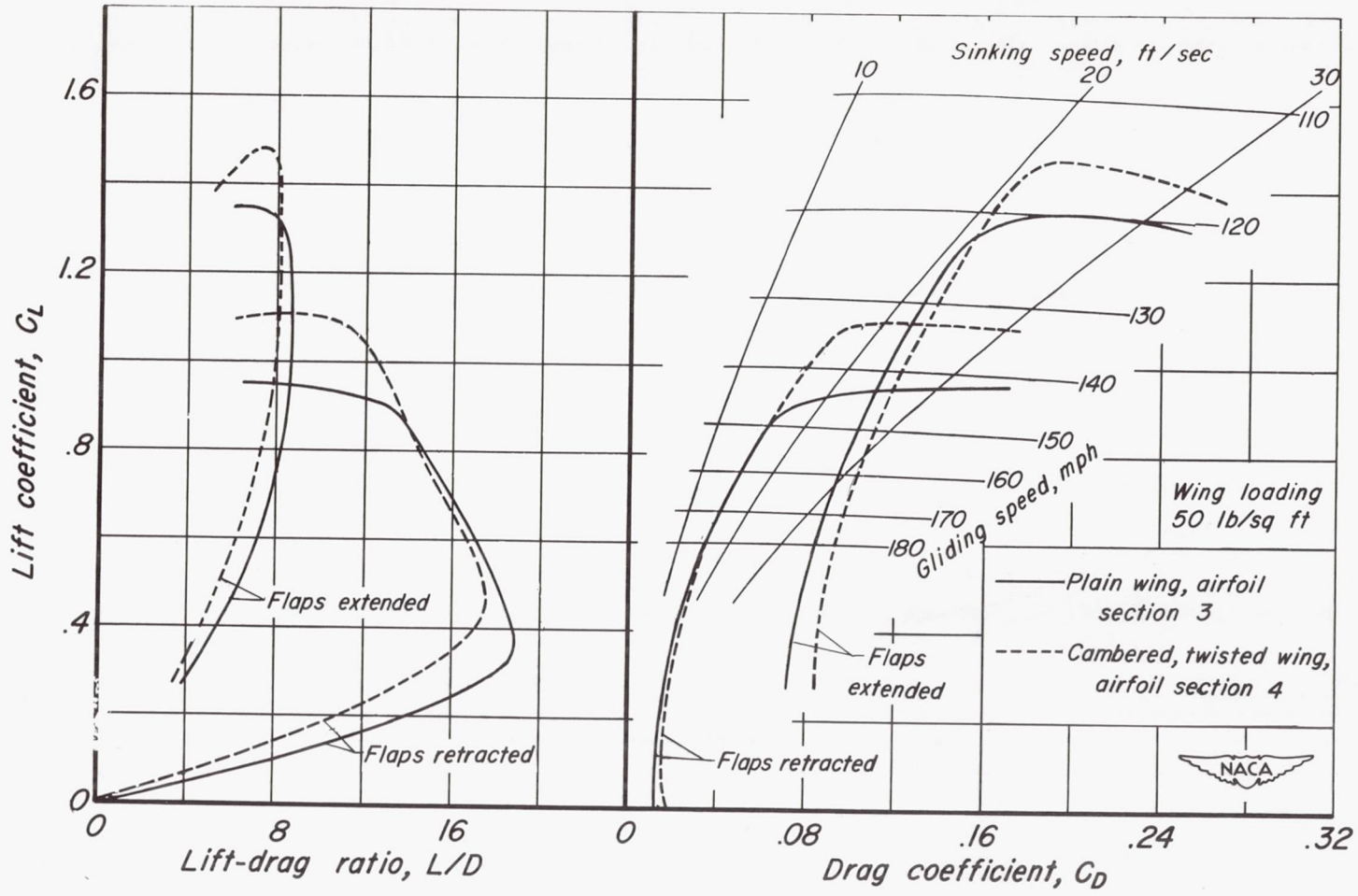

Figure 8.– The lift-drag ratio and power-off glide characteristics of the plain wing model with the cambered leading edge and the cambered, twisted wing model with the modified leading edge (0.015c L.E. radius).

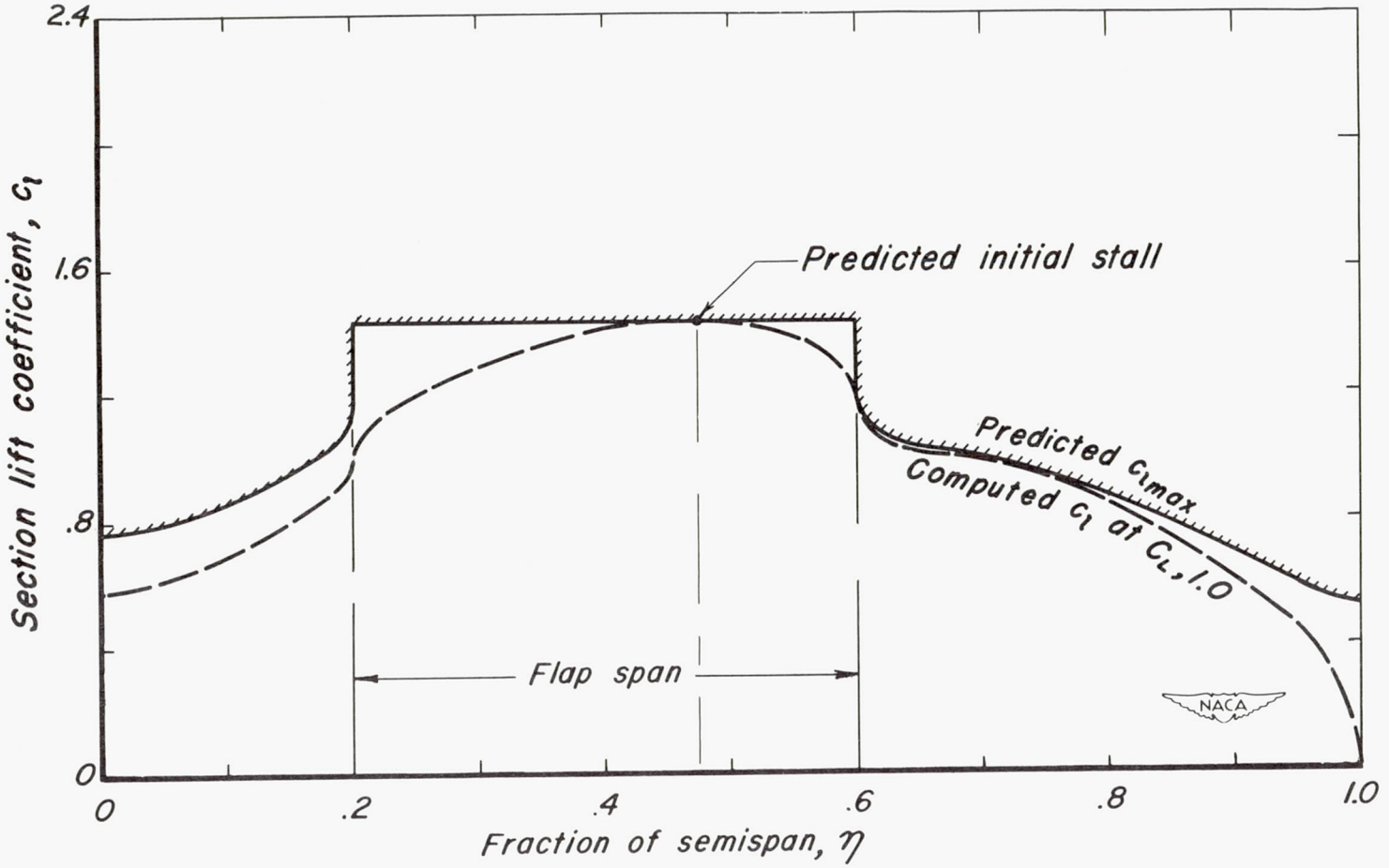

(a) Plain wing with flaps extended.

Figure 9.– Predicted maximum span loadings without flow separation.

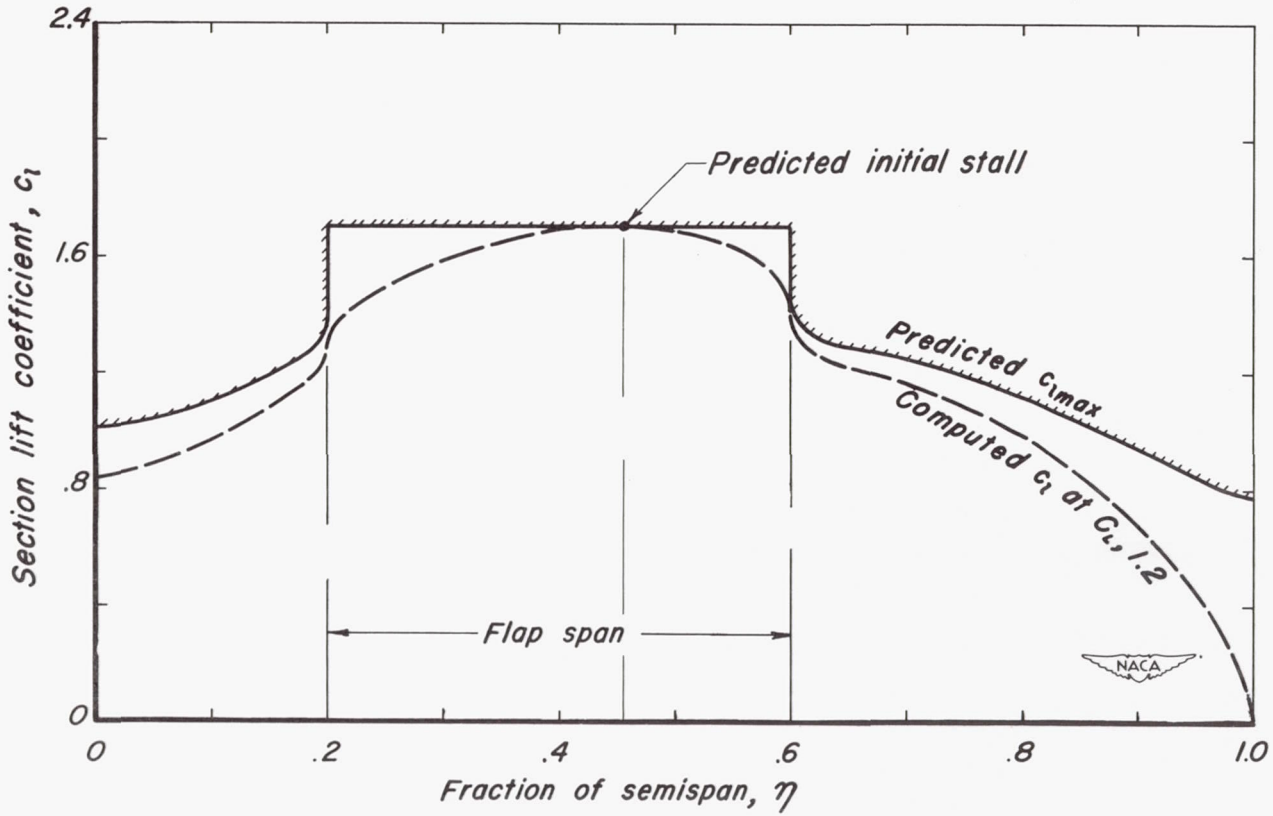

(b) Cambered, twisted wing with flaps extended.

Figure 9.- Concluded.